Medical Engineering and Physics 68 (2019) 65–75

Contents lists available at ScienceDirect

Medical Engineering and Physics

journal homepage: www.elsevier.com/locate/medengphy

A predictive computational model to estimate myocardial temperature during intracoronary hypothermia in acute myocardial infarction

Bettine G. van Willigen[a,*], Luuk C. Otterspoor[b], Marcel van 't Veer[a,b], Tilaï T. Rosalina[a], Nico H.J. Pijls[a,b], Frans N. van de Vosse[a]

[a] Department of Biomedical Engineering, Eindhoven University of Technology, The Netherlands
[b] Department of Cardiology, Catharina Hospital Eindhoven, The Netherlands

ARTICLE INFO

Article history:
Received 9 July 2018
Revised 15 March 2019
Accepted 31 March 2019

Keywords:
Acute myocardial infarction
Myocardial hypothermia
Lumped
Parameter model

ABSTRACT

Hypothermia, if provided before coronary reperfusion, reduces infarct size in animal models of acute myocardial infarction (AMI). Translation to humans has failed so far, because the target temperature is not reached in time within the endangered myocardium using systemic hypothermia method. Hence, a clinically applicable method has been developed to provide intracoronary hypothermia using cold saline, selectively infused locally into the infarct area.

In this study, a lumped parameter model has been designed to support the clinical method and to describe this myocardial cooling process mathematically. This model is able to predict the myocardial temperature changes over time, which cannot be measured, based on the temperature and flow of the intracoronary injected cold saline and coronary arterial blood. It was validated using data from an isolated beating porcine heart model and applied on data from patients with AMI undergoing intracoronary hypothermia.

In prospect, the computational model may be used as an assistive tool to calculate the patient specific flow rate and temperature of saline required for reliable achievement of the target myocardial temperature in the hypothermia enhanced clinical treatment of AMI.

1. Introduction

Despite important gains in survival in the last decades, coronary artery disease, especially acute myocardial infarction (AMI), remains the leading cause of death in the world [1–5]. In AMI patients, infarct size relates directly to short- and long-term mortality and to the development of chronic heart failure [6–8]. Therefore, limiting infarct size is of paramount importance. To reduce infarct size, the preferred therapy of AMI is timely reperfusion by primary percutaneous coronary intervention (PPCI) [9]. Although reperfusion is essential to save myocardium, the process of restoring blood flow to the ischemic area can induce different forms of myocardial injury and cardiac myocyte death: a phenomenon known as myocardial reperfusion injury [10–12]. Myocardial reperfusion injury may even account for up to 50 percent of the total infarct size after intervention [13]. Currently, there is no effective therapy to reduce myocardial reperfusion injury in humans [14,15].

In experimental studies, it has been shown that mild hypothermia ($32-34\,^{\circ}C$) induced before the onset of reperfusion (i.e. during occlusion of the coronary artery) attenuates myocardial reperfusion injury, thereby reducing infarct size [16–22]. However, systemic cooling methods investigated in humans have been disappointing so far [23–27] probably because the myocardial area at risk (AAR) did not reach the target temperature quick enough [28]. Therefore, a clinical applicable intracoronary cooling method was developed in which hypothermia can be applied selectively to the infarct area by infusing cold saline before reperfusion (occlusion phase) and after reperfusion (reperfusion phase) [29,30].

This method was first tested in an isolated beating porcine heart model of AMI, in which local cooling of the myocardial AAR was successfully achieved, while having direct feedback on coronary temperature by a pressure/temperature sensor-tipped wire in the distal coronary artery. Furthermore, the temperature of the myocardial AAR was measured with needle thermistors at three locations [31]. When applying this method to humans, the myocardial needle thermistors are evidently absent and only the intracoronary sensor is present. Therefore, there is an unmet need for a model that can predict the temperature of the myocardial AAR by the measured intracoronary temperature.

* Corresponding author.
E-mail address: b.g.v.willigen@tue.nl (B.G. van Willigen).

https://doi.org/10.1016/j.medengphy.2019.03.011
1350-4533/

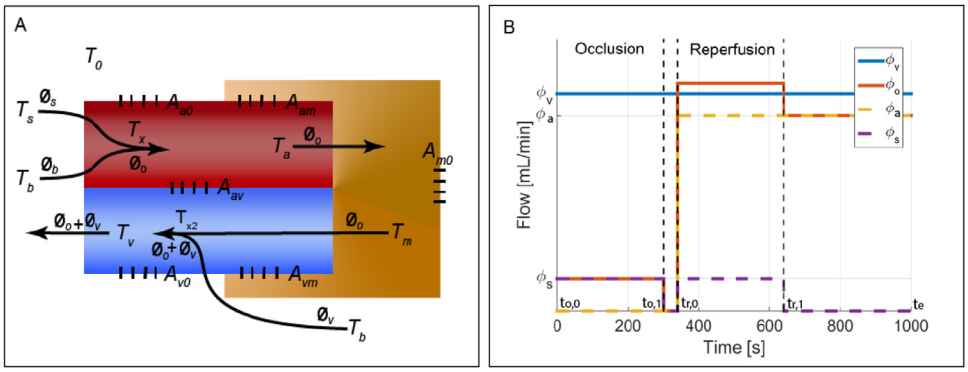

Fig. 1. (A) Schematic overview of the numerical model with three compartments: the arterial side (red), the myocardial AAR (bronze), and the venous side (blue). Heat transfer caused by convection and conduction is indicated with arrows and black parallel dashes, respectively. The symbols are explained in the mathematical equations described in Sections 2.1.1–2.1.3 (B) The venous flow (ϕ_v, blue), saline and blood flow combined (ϕ_o, orange), arterial blood flow (ϕ_a, yellow), and saline flow (ϕ_s, purple) input over time with the occlusion phase ($t_{o,0} < t < t_{o,1}$), the reperfusion phase ($t_{r,0} < t < t_{r,1}$), and after the cooling period ($t_{r,1} < t < t_e$). (For interpretation of the references to color in this figure legend, the reader is referred to the web version of this article.)

In other words, the purpose of this study is to design a computational model, which is able to predict the myocardial temperature based on the intracoronary arterial temperature and the temperature and flow of the injected saline. In future clinical studies of AMI patients treated with intracoronary hypothermia, this model also may be used as an assistive tool to calculate the patient specific saline infusion rate and temperature requirements needed to achieve an optimal therapeutic myocardial temperature for each individual patient.

2. Methodology

2.1. Theoretical background

Assuming that a global distribution of blood flow, pressure, and heat transfer is sufficient to describe the temperature distribution in the coronary circulation, a lumped parameter model is used to describe the temperature response in the coronary circulation during the cooling period before reperfusion (occlusion phase) and after reperfusion (reperfusion phase).

The model consists of three compartments: 1) the coronary artery (red) representing the infarct related coronary artery distal to the occlusion and the arterial side of the microcirculation, 2) the myocardial AAR (bronze), and 3) the coronary vein (blue) representing the venous side of the microcirculation and the assembly of all coronary veins (Fig. 1A). In addition, the boundary of every compartment, or ambience (white area), is set to body temperature (T_0). For complete understanding, in the sequel of this section, the compartments are described individually.

2.1.1. The coronary arterial temperature response

The first compartment, the arterial side of the coronary circulation, has an inflow of saline (ϕ_s) and arterial blood (ϕ_a) with temperature T_s and T_b, respectively, which results in a different total inflow (ϕ_o) during the occlusion and reperfusion phase (Fig. 1B).

If we neglect entropy of mixing effects and assume constant heat capacity in the temperature range of interest, these two flows mix to a temperature T_x:

$$T_x = \frac{\phi_s c_s T_s + \phi_a c_b T_b}{\phi_s c_s + \phi_a c_b} \tag{1}$$

With c_b and c_s the specific heat capacity of blood and saline $[\frac{J}{kg \cdot K}]$, respectively.

Furthermore, conductive heat transfer (Fig. 1A, black dashes) occurs between: 1) artery and ambience 2) artery and myocardium, and 3) artery and vein with the thermal resistances R_{a0}, R_{am}, and R_{av}, respectively. The mathematical description of the coronary artery temperature response is as follows:

$$\frac{dT_a}{dt} = \frac{1}{C_a}(\phi_o \rho_x c_x (T_x - T_a) - \frac{1}{R_{a0}}(T_a - T_0) + -\frac{1}{R_{am}}(T_a - T_m) - \frac{1}{R_{av}}(T_a - T_v)) \tag{2}$$

Where $C_a = V_a \rho_b c_b$ with C_a the coronary arterial thermal capacitance $[\frac{J}{K}]$, V_a the volume of the coronary artery $[m^3]$, and ρ_b the density of blood $[\frac{kg}{m^3}]$. Furthermore, the thermal resistances $R_i = \frac{d_i}{A_i * k_m}$ with $i = \{a0, am, av\}$, d_i a representative heat transfer thickness, A_i a representative heat transfer surface area, and k_m the thermal conductivity of the myocardium. Finally, ρ_x and c_x are the density $[\frac{kg}{m^3}]$ and specific heat capacity $[\frac{J}{kg \cdot K}]$ of the mixture of blood and saline, respectively.

2.1.2. The myocardial temperature response

The mixture of blood and saline leaves the coronary artery with temperature T_a and flow ϕ_o into the AAR, where conductive heat transfer takes place between: 1) coronary artery and myocardium, 2) myocardium and ambience, and 3) vein and myocardium with the thermal resistance R_{am}, R_{mv}, and R_{m0}, respectively. The mixture of blood and saline leaves the myocardium with temperature T_m and flow ϕ_o. This results in:

$$\frac{dT_m}{dt} = \frac{1}{C_m}(\phi_o \rho_x c_x (T_a - T_m) + \frac{1}{R_{am}}(T_a - T_m) + -\frac{1}{R_{mv}}(T_m - T_v) - \frac{1}{R_{m0}}(T_m - T_0)) \tag{3}$$

Where $C_m = m * c_t$ with C_m the myocardial thermal capacitance $[\frac{J}{K}]$, m the mass of the AAR $[kg]$, and c_t the specific heat capacity of myocardial tissue $[\frac{J}{kg \cdot K}]$. $R_i = \frac{d_i}{A_i * k_m}$ with $i = \{am, mv, m0\}$ are again the thermal resistances.

2.1.3. The venous temperature response

Subsequently, blood is flowing with ϕ_o to the venous side with temperature T_m merging with another blood flow ϕ_v, which originates from other parts of the myocardium than the AAR. These two flows mix to temperature T_{x2} and enter the vein:

$$T_{x2} = \frac{\phi_v c_b T_b + \phi_o c_b T_m}{\phi_v c_b + \phi_o c_b} \tag{4}$$

Conductive heat transfer occurs between: 1) myocardium and vein 2) vein and ambience, and 3) artery and vein with the thermal resistances R_{mv}, R_{v0}, and R_{av}, respectively, resulting in:

$$\frac{dT_v}{dt} = \frac{1}{C_v}((\phi_v + \phi_o)\rho_x c_x(T_{x2} - T_v) + \frac{1}{R_{mv}}(T_m - T_v) + -\frac{1}{R_{v0}}(T_v - T_0) + \frac{1}{R_{av}}(T_a - T_v)) \quad (5)$$

Where $C_v = V_v \rho_b c_b$ with C_v the venous thermal capacitance $[\frac{J}{K}]$ and V_v the volume of the vein $[m^3]$ and $R_i = \frac{d_i}{A_i * k_m}$ with $i = \{mv, v0, av\}$ the thermal resistances for the venous temperature response.

The initial temperatures (T_a, T_m, and T_v) are set on body temperature and to maintain simplicity, ρ_x and c_x are assumed to have the same value as ρ_b and c_b, respectively.

The flow inputs depend on the phase as shown in Fig. 1B: saline (purple) flows during both phases (occlusion and reperfusion phase), while arterial blood (yellow) flows only during the reperfusion phase and venous blood (blue) flows constantly.

2.2. Parameter estimation

The model is implemented in MATLAB R2015b and the ordinary differential equations describing the arterial $[T_a]$ and myocardial $[T_m]$ temperature response are solved with the MATLAB solver ode15s. The venous temperature $[T_v]$ is not measured in humans. Therefore, not included with parameter estimation and fixed on T_b.

For the estimation of the parameters, the MATLAB non-linear least squares function (lsqnonlin) is used, such that the sum of squared errors (χ) between the experimental data (y) and the simulation of the model ($f(\underline{x})$) is minimized:

$$\chi = \sum_{i=1}^{n}(y_i - f_i(\underline{x}))^2 \quad (6)$$

In our model, y equals the measured coronary arterial temperature (see next paragraphs), $f(\underline{x})$ equals the simulation of the model, T_a, with the estimated parameters $\underline{x} = \{m, A_{a0}, A_{am}, A_{av}, A_{m0}, A_{mv}, A_{v0}, V_a, V_v, \phi_v\}$, and i the data points (sample frequency of 100 per second.). The parameters $\underline{x}$ remain the same value despite the phase. In contrast, ϕ_a is assumed zero during the occlusion phase ($t_{o,0} < t < t_{o,1}$) and changes during the reperfusion phase ($t_{r,0} < t < t_{r,1}$) (Fig. 1B). Therefore, the parameters $\underline{x}$ are first estimated on the occlusion phase. Thereafter, ϕ_a is fitted on the reperfusion phase with the parameters $\underline{x}$ fixed.

This method seeks for an optimal combination of parameters describing the measured data with minimal error, the optimal parameter vector. It is possible that the method obtains a local minimum, while there exists a global minimum in the parameters space. Therefore, an initial parameter space of 100 samples is generated based on Latin Hypercube Sampling (LHS) within a physical realistic range obtained from literature (see Appendix A). The method runs 100 times based on different initial parameters to reduce the probability of finding a local minimum.

2.3. Data

In this study, two datasets are used: 1) a dataset to validate the model obtained from isolated porcine beating hearts, which contains intracoronary, myocardial, and venous temperatures of five experiments [31] and 2) a dataset to apply the model obtained from the clinical SINTAMI study [29] containing intracoronary temperature and aortic (P_a) and distal coronary (P_d) pressure of 10 patients. This section gives a brief description of the procedures used to obtain these data.

2.3.1. Isolated beating porcine hearts

A full description of the isolated beating porcine heart model of AMI is described by Otterspoor et al. [31,32]. In short, five porcine hearts temperatures were obtained at six locations: in the distal coronary artery (distal T artery, T_a^{meas}), three myocardial positions throughout the AAR (T infarct) with T_m^{meas} as mean of the three positions, at a position outside the AAR (T reference), and the great cardiac vein (T vein, T_v^{meas}) (Fig. 2). These temperatures were measured during the occlusion phase created by inflating an over-the-wire-balloon (OTWB, Apex™, Boston Scientific, 12 mm, 2.5–3.5 mm) in the mid segment of left anterior descending artery (mid-LAD) and reperfusion phase after deflating the OTWB.

During both phases, saline was infused through its lumen selectively into the AAR at a rate of 30 mL/min for 5 min. with a temperature of 22 °C and 4 °C for the occlusion and reperfusion phase, respectively.

The porcine dataset underwent small adjustments to synchronize the occlusion and reperfusion phases of the five porcine experiments. After the synchronization, T_a^{meas}, T_m^{meas}, and T_v^{meas} were averaged for the five experiments. The average T_a during the occlusion phase was used to estimate the model parameters described in Section 2.2. The parameter estimation is performed on the mean rather than on each realisation to avoid fitting on outliers. These fitted parameters are used to predict the T_m. The validation consisted of the comparison of T_m^{meas} with the predicted values, T_m.

2.3.2. Clinical study: SINTAMI

The Safety and feasibility of INTracoronary hypothermia in Acute Myocardial Infarction study (SINTAMI), assessed safety and feasibility of the intracoronary hypothermia method in humans [33]. In this study, 10 patients with AMI were included (all provided with written informed consent). An OTWB (Apex™, Boston Scientific, USA) was placed at the location of the occlusion. During the occlusion and reperfusion phase, saline of 22 °C and 4 °C, repectively, was infused. After both phases, both performed for a maximum of 10 min, the saline flow stopped and regular PPCI procedure followed. The aortic (P_a) and distal coronary (P_d) pressure and intracoronary temperature (T_a) distal to the occlusion were monitored. Alterations in saline flow during the experiments will result in peaks in T_a^{meas}. In the model, these peaks are neglected, but the alterations in flow are included.

In patients, the coronary artery may recoil after reperfusion at the location of the occlusion causing AMI, which increases the resistance of the stenosis (R_s). Furthermore, despite the effort to reduce the edema, the swelling will not be completely gone, which results in an increase of the resistance of the microcirculation (R_m). The increase of R_m and R_s result both in a decrease of P_d. Consequently, the flow $\phi_a(t)$ with $t_{r,0} < t < t_{r,1}$ (Fig. 1B) is related to P_d, R_s, and R_m, which both vary in time:

$$\phi_a(t) = \frac{P_a(t) - P_d(t)}{R_s(t)} = \frac{P_d(t) - P_v(t)}{R_m(t)} \quad \text{with} \quad t_{r,0} < t < t_{r,1} \quad (7)$$

With assumption that the venous pressure $P_v << P_d$ and using the right side of (7), this yields:

$$\phi_a(t) = \frac{P_d(t) - P_v(t)}{R_m(t)} = \frac{P_d(t)}{R_m(t)} \quad \text{with} \quad t_{r,0} < t < t_{r,1} \quad (8)$$

As mentioned, R_m is related to P_d; therefore, R_m is described as follow:

$$R_m(t) = R_m(t_{r,0})\frac{\bar{P_a}}{P_d(t)} \quad \text{with} \quad t_{r,0} < t < t_{r,1} \quad (9)$$

With $R_m(t_{r,0}) = \frac{\bar{P_a}}{\phi_a(t_{r,0})}$ and $\phi_a(t_{r,0})$ representing the flow just after revascularisation (at t = $t_{r,0}$). Substituting (9) in (8) results in:

$$\phi_a(t) = \left(\frac{P_d(t)}{\bar{P_a}}\right)^2 \phi_a(t_{r,0}) \quad \text{with} \quad t_{r,0} < t < t_{r,1} \quad (10)$$

In summary, the flow has a linear relation with pressure and resistance (8), but the resistances (R_m and R_s) change over time.

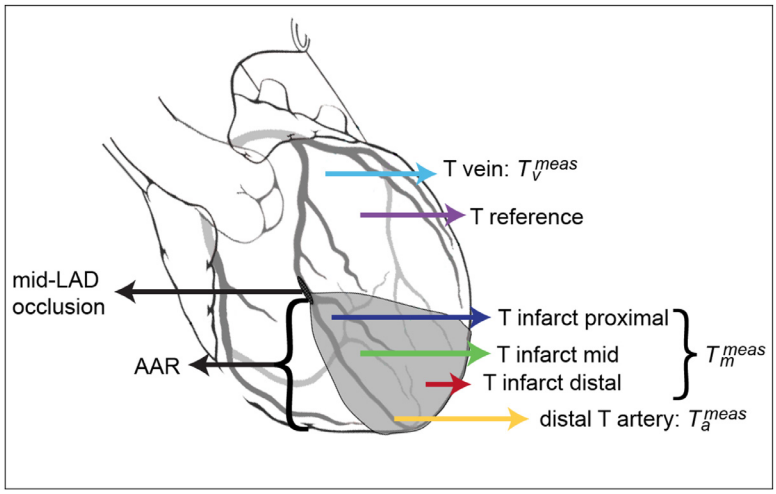

Fig. 2. Overview of the thermistor position: The grey zone indicates the AAR. The black oval indicates the site of occlusion in the LAD. T infarct proximal: thermistor close to the site of the LAD occlusion; T infarct mid: thermistor at the mid infarct area; T infarct distal: thermistor at the distal infarct area; T_m^{meas} is the mean of the three thermistors. T reference: thermistor in the non-infarcted myocardium; T vein: thermistor in the proximal great cardiac vein, T_v^{meas}. In addition, T distal artery: the guidewire with temperature sensor is present within the distal lumen of the coronary artery, T_a^{meas}.

Therefore, the flow is approximated with the quadratic decrease of P_d based on experimental observations.

The SINTAMI data is used as a proof of concept. The T_a^{meas} during the occlusion phase is used to fit T_a. Subsequently, the fitted parameters (described in Section 2.2) are used to predict T_m. To demonstrate its feasibility, T_m will be checked whether it is realistic.

2.4. Sensitivity analysis

In order to make the model patient specific, it is important to identify the parameters with the most influence on the outcome, such that these parameters could be coupled to patient data. To identify the important parameters, the variance based sensitivity analysis (VBSA) is applied on the model. This method is widely used, because it is global, quantitative, model free, and easy to interpret and implement [34,35]. Furthermore, VBSA is able to identify parameters, which can be fixed in their uncertainty range (Factor Fixing) and finds the importance ranking amongst the parameters (Factor Prioritization). The VBSA suggest that the total variation of the output can be fractionated in the variation of the individual parameters and their interactions [34,35]. A parameter with a large contribution to the variance of the total output, identified with a high main sensitivity index (S_M), should be measured as accurately as possible to reduce the total variance of the output. The purpose of S_M is Factor Prioritization. A parameter with a small contribution to the total variance of the output, including its interactions, could be fixed in its uncertainty range, because the outcome of the output would not depend on this parameter within this range. These are the parameters with a low total sensitivity index (S_T). The indices are computed based on an approximation method of Saltelli [36].

3. Results

3.1. Porcine beating hearts

The validation of the model is described in Fig. 3. The mean T_a^{meas} and T_m^{meas} of the five porcine experiments (mean ± standard deviation, sd) are shown in dark and light grey, respectively. The T_m^{meas} decreases by $5.5 \pm 2.6\,^{\circ}C$ (mean ± sd) and $4.1 \pm 0.9\,^{\circ}C$ during occlusion and reperfusion phase, respectively. The T_a^{meas} decreases by $12.0 \pm 0.5\,^{\circ}C$ and $5.0 \pm 1.7\,^{\circ}C$ during occlusion and reperfusion phase, respectively.

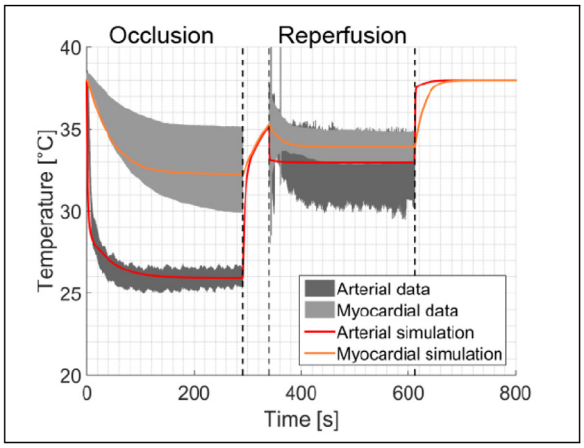

Fig. 3. The mean ± the sd of the arterial (dark grey) and myocardial (light grey) temperature of the five experiments and the arterial (red) and myocardial (orange) simulation, in which the parameters are fitted on the mean of the arterial data of the five experiments. (For interpretation of the references to color in this figure legend, the reader is referred to the web version of this article.)

The model parameters were fitted on the T_a^{meas} during the occlusion phase (Fig. 3, red line, occlusion phase). With this parameter set the T_a^{meas} during the reperfusion phase (red line, reperfusion phase) was predicted within the measured range (dark grey) by fitting ϕ_a on the reperfusion phase. Moreover, the predicted T_m (orange line) follows the measured data (light grey) for both phase as well (Fig. 3). In addition, both temperature responses return to body temperature, when saline stopped. Finally, the fitted parameters are within a physiologically realistic range Table 1, except for the values of the arterial and venous area of the microcirculation, which will be discussed in the discussion.

3.2. Clinical study

Complete datasets were obtained for 7 out of the 10 patients; therefore, only these 7 patients are used in this study. The simulation of these patients are presented in Appendix B. Fig. 4 shows the arterial (red) and myocardial (orange) temperature response simulated by the model with parameters fitted on the arterial data (dark grey) during occlusion phase and ϕ_a on the reperfusion phase of Patient 2 as example. As can be seen, during the occlusion

Table 1
Estimated parameters based on the mean arterial data of the five porcine experiments and physiologically realistic range obtained from literature (Appendix A Table A.4).

Parameter	Fitted value	Range
m[kg]	$7.00 \cdot 10^{-2}$	[0.70 1.30] $\cdot 10^{-1}$
A_{a0}[m^2]	$6.28 \cdot 10^{-5}$	[0.63 9.42] $\cdot 10^{-4}$
A_{am}[m^2]	$3.05 \cdot 10^{-2}$	[1.31 4.06]
A_{av}[m^2]	$3.14 \cdot 10^{-5}$	[0.31 4.71] $\cdot 10^{-4}$
A_{m0}[m^2]	$6.45 \cdot 10^{-3}$	[0.65 1.20] $\cdot 10^{-2}$
A_{mv}[m^2]	$1.10 \cdot 10^{-2}$	[1.31 4.06]
A_{v0}[m^2]	$6.28 \cdot 10^{-5}$	[0.63 9.42]$\cdot 10^{-4}$
V_a[mL]	1.88	[1.01 1.88]
V_v[mL]	2.40	[2.40 4.45]
ϕ_a[mL/min]	$1.85 \cdot 10^{2}$	[50 300]
ϕ_v[mL/min]	$5.00 \cdot 10^{1}$	[50 300]

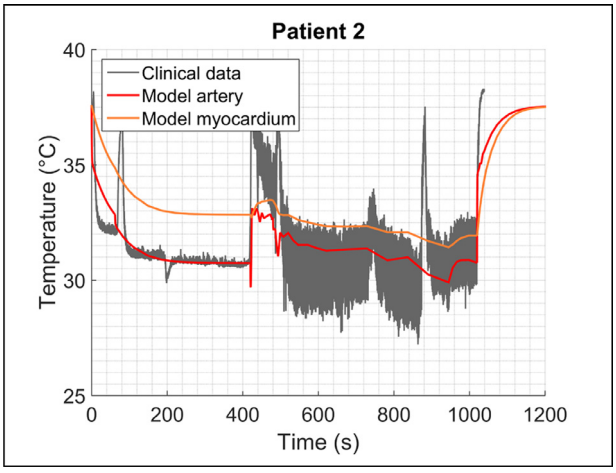

Fig. 4. The intracoronary arterial data (grey) temperature response and the simulation of the intracoronary arterial temperature (red) and the prediction of the myocardial (orange) temperature. (For interpretation of the references to color in this figure legend, the reader is referred to the web version of this article.)

Table 2
The mean of the fitted parameters on the arterial temperature during occlusion phase of the SINTAMI data of the 7 patients and their physiologically range. The parameters per patient are shown in (Appendix C, Table C.6).

Parameter	Fitted mean	Range
m[kg]	$4.63 \cdot 10^{-2}$	[4.00 8.00] $\cdot 10^{-2}$
A_{a0}[m^2]	$8.85 \cdot 10^{-5}$	[0.63 9.42] $\cdot 10^{-4}$
A_{am}[m^2]	$9.16 \cdot 10^{-2}$	[0.75 2.50]
A_{av}[m^2]	$3.22 \cdot 10^{-5}$	[0.31 4.71] $\cdot 10^{-4}$
A_{m0}[m^2]	$4.98 \cdot 10^{-3}$	[3.68 7.37] $\cdot 10^{-3}$
A_{mv}[m^2]	$2.98 \cdot 10^{-2}$	[0.75 2.50]
A_{v0}[m^2]	$2.86 \cdot 10^{-4}$	[0.63 9.42]$\cdot 10^{-4}$
V_a[mL]	1.15	[0.58 1.16]
V_v[mL]	1.59	[1.37 2.74]
ϕ_a[mL/min]	165	[50 300]
ϕ_v[mL/min]	160	[50 300]

phase (0–420 s), the T_a^{meas} drops quickly within 60 s. Thereafter, the reperfusion phase starts with a larger oscillation of the T_a^{meas} due to the increased coronary blood flow. As aimed for, the T_m^{meas} drops to approximately the same temperature during the reperfusion phase for the occlusion phase. Furthermore, the figure shows that T_a (red line) is very well simulated and T_m (orange line) is realistic.

In addition, the parameters of the 7 patients are within the physiological range. The mean of the parameters of the 7 patients are shown in Table 2. The parameters per patient are shown in (Appendix C, Table C.6).

3.3. Sensitivity analysis

The VBSA is applied on the model with the sum of squared error, χ, as output (6). The parameters are estimated based on the arterial data ($y = [T_a^{meas}]$) during the occlusion phase. Furthermore, the number of realizations is $N = 1000k$ with k the number of parameters. Fig. 5 shows the mean S_M (A) and the total S_T (B) index of the 11 parameters. The parameter with the largest contribution to the variance of the total output is A_{am} (the area between the arterial and myocardial compartment) (Fig. 5A). Fig. 5B shows that the parameters A_{v0}, V_a, and V_v can be fixed in their uncertainty range due to their low S_T. The arterial flow ϕ_a also has a low S_T, because of its value of zero during the occlusion phase. The other parameters (m, A_{a0}, A_{av}, A_{m0}, A_{vm}, and ϕ_v) show a small S_m and a larger S_T, which means that their interactions are important.

4. Discussion

To mathematically describe myocardial hypothermia, a model of heat distribution per compartment was developed. This model is able to describe the cooling process and the trend of both the arterial and myocardial temperature curves obtained from the isolated beating porcine heart of myocardial infarction. In humans it is not possible to measure the actual myocardial temperature in the AAR, in contrast to the isolated beating porcine heart. Hence, the model is necessary to predict a realistic myocardial temperature.

First, the model is verified on data of porcine beating hearts [31]. As shown in Fig. 3, the predicted myocardial temperature follows the trend of the corresponding data when the model parameters are fitted on the measured arterial temperature data during the occlusion phase.

Otterspoor et al. [31] mentioned the study limitations for the porcine beating heart experiments concerning the study set up and the anatomic differences between pig and human. A difficulty in the porcine experiments for this study was the large variation in myocardial temperatures between the experiments during the occlusion phase, which hampered an unambiguous estimation of the model parameters. During the occlusion phase, heat transfer mainly occurs by conduction, which leads to a less homogenously distribution of heat than convection dominated heat transfer. Placing the thermistors visually in combination with the complexity of the coronary circulation, leads to a wide spread in myocardial temperatures during the occlusion phase between the experiments. Nevertheless, Fig. 3 shows that the model is able to simulate the trend of the myocardial temperature very well. However, in order to determine a more precise myocardial temperature during the occlusion phase based on the intracoronary arterial temperature, more myocardial data is necessary.

In contrast, the reperfusion phase is dominated by convection, which results in a homogenously dispersion of the cooling; therefore, the myocardial temperature depends less on the location of the thermistors and the arrangment of the coronary vessels. This results in similar arterial and myocardial temperature responses during the reperfusion phase and a more accurate simulated myocardial temperature during the reperfusion phase.

Notably, during the occlusion phase, there is a large difference between the myocardial and arterial temperature, while during the reperfusion phase, these temperatures are about the same. This is caused by the different heat exchange during both phases. During the occlusion phase, the flow is slow, which results in heat exchange mainly by conduction. This results in a temperature gradient from the artery to the myocardium. In contrast, the flow during the reperfusion phase is higher. Therefore, convection is dominating, which results in similar arterial and myocardial temperatures. The model is able to describe this phenomenon.

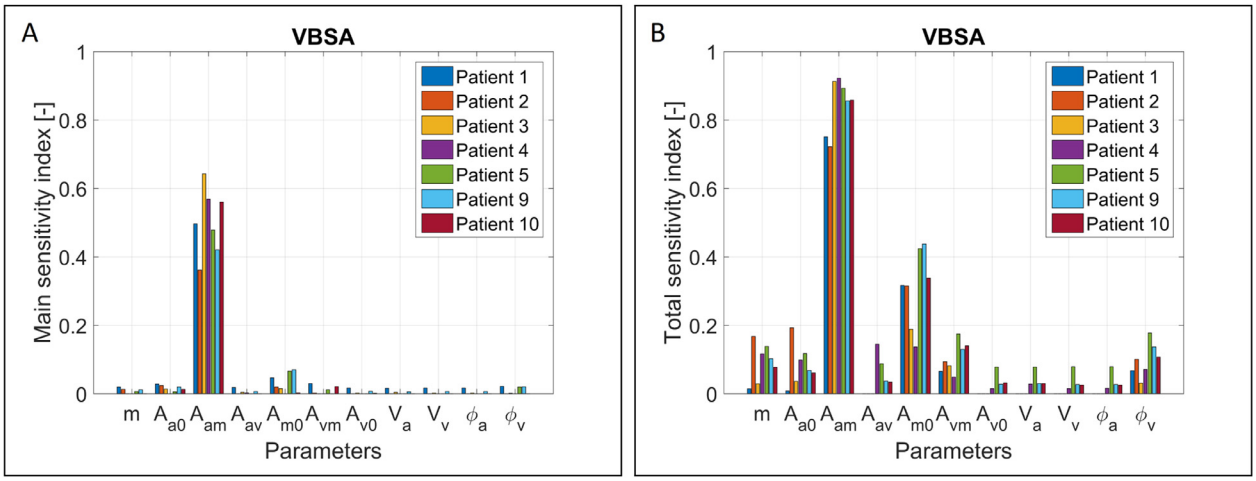

Fig. 5. The main (A) and total (B) sensitivity index of VBSA with N = 1000k realisations and parameters estimated on the arterial data during the occlusion phase.

The determination of the parameters concerning the resistance of the myocardium (determined by A_{am} and A_{mv}) was not within the predefined physiological range. This parameter range is based on experiments on dogs, which have many collaterals unlike pigs. This lack of vascularization results in a higher resistance of the myocardium (lower A_{am} and A_{mv}) in pigs, because the heat of the myocardium has more difficulty to reach the artery. This is also shown in the significant distinction between myocardial and arterial temperature during the occlusion phase due to a very low arterial temperature Fig. 3. However, the exact increase of resistance described with the values of A_{am} and A_{mv} is unknown, which could explain the low values of A_{am} and A_{mv}.

Secondly, the model is applied on patient data from the SINTAMI study [33].To overcome the negative results of mild hypothermia in human studies probably due to systemic cooling [28], selectively intracoronary infusion of saline can potentially make hypothermia clinically applicable. As shown previously [29,33], the cooling is restricted to the jeopardized myocardium, achieved quickly, and maintained. In Fig. 4, the prediction of myocardial temperature is shown to be realistic when the parameters are fitted on the arterial temperature data of the occlusion phase.

The data obtained from the clinical study contains the intracoronary arterial temperature response, P_a, and P_d (Appendix B). In contrast to the porcine experiments, the saline flow (14–30 mL/min) was adjusted during the procedure to control the decrease of arterial temperature. The P_a and P_d give an indication if both phases were successful. During the occlusion phase, P_d should be significant lower than P_a due to the coronary occlusion and should restore to approximately the same value as P_a during reperfusion. The model succeeds in simulating the different relation between the arterial and myocardial temperature for different P_d.

The amount of similarity between the arterial and myocardial temperature depends on the blood flow. The larger the blood flow, the more heat transfer by convection, the more similar the arterial and myocardial temperature response.

For the porcine experiments, blood flow was completely restored after deflating the OTWB, i.e. the P_d is about equal with P_a, while for the patients, the P_d diminishes. Therefore, more conductive heat transfer takes place during the reperfusion phase, which results in a less similar arterial and myocardial temperature response. The patients with a large distinction between the myocardial and arterial temperature (Appendix C) show, indeed, a low P_d, e.g. patient 3 and 10 (Appendix B).

There has been chosen for a simplification by using a lumped parameter model. As mentioned above, the myocardial temperature may and probably will depend on the location and depth of the thermistors. Therefore, the myocardial temperature was measured at three different locations (Fig. 2) and the average of these temperatures was used for simulation to decribe the trend of the temperature rather than the absolute value. Therefore, spatial variations inside the components are unneccessary. In addition, the specific heat and the density of the entrance flow into the artery is assumed to be equal to the specific heat of blood, while the entrance fluid is a mixture of blood and saline. Therefore, the specific heat and the pressure is time dependent and depends on the amount of flow of saline and blood and the amount of blood already in the compartment. The density of saline (1004.6 kg/m^3) is less than 5% smaller than the density of blood [10]; therefore, can be assumed to be equal. The specific heat of saline (4190 $\frac{J}{kgK}$) is approximately 13% larger than the specific heat of blood (3651 $\frac{J}{kgK}$). This linearization is sufficient for the reperfusion phase, because the blood flow is at least three times larger than the saline flow. However, during the occlusion phase, only saline is entering the vessel and mixes with an unknown amount of blood distal to the occlusion. Therefore, the entrance fluid during the occlusion phase would have a specific heat more towards that of saline than that of blood. A higher specific heat means that more heat is needed to change the temperature, which would lead to a lower arterial temperature than is simulated with the current model. This could improve the simulation of the porcine data and the results of patient 5 and 9, for which the simulated arterial temperature during the occlusion is slightly higher than the data (Appendix C).

In addition, the saline flow should replace the coronary blood flow partly during reperfusion phase, because of the assumption of hyperemia. However, the model adds the saline flow to the blood flow during the reperfusion phase to avoid time depending parameters (Fig. 1B). Furthermore, the model is applied on AMI patients with occlusions in the LAD. Although it is expected that the temperature response can be simulated for occlusions in other coronary arteries with parameters adjusted to the size and location of the occlusion, this should be further examined.

The sensitivity analysis is performed to indicate the parameters, which should be measured accurately (high S_M) and which can be fixed in their uncertainty range (low S_T). The VBSA identifies a high S_M for A_{am}, which would make the model more accurate when it is measured precisely. Furthermore, A_{v0}, V_a, and V_v are not influencing the outcome of the model within their uncertainty range and they can, therefore, be fixed. This would make the simulation of the temperature response faster. It has been assumed that the number of simulations are sufficient to determine the sensitivity indices; however, a bootstrapping method should confirm this

assumption. Finally, the sensitivity analysis resulted in one important parameter, A_{am}; therefore, this model is ideal for personalized planning of treatment. For instance, this parameter could be coupled to myocardial mass as the relation described in [37].

5. Conclusion

In conclusion, the computational model is designed to describe heat distribution within the coronary circulation based on three compartments (artery, myocardium, and vein). This model is able to simulate the arterial temperature with a realistic predicted myocardial temperature. In an ongoing, randomized clinical proof of principle trial of intracoronary hypothermia in patients with acute myocardial infarction (EURO-ICE study; ClinicalTrials.gov, registration number: NCT03447834), the computational model can be further refined. Thereafter, it is plausible that the model may play a role in clinical practice in patients undergoing intracoronary hypothermia for AMI by computing a patient specific flow and temperature of the saline to be infused.

Conflict of interest

N. Pijls receives institutional research grants from and is a consultant for St. Jude Medical. The other authors have no conflicts of interest to declare.

Funding

None.

Ethical approval

Not required.

Table A3
Minimum and maximum value of the characteristics of mid-LAD and capillaries.

Characteristics	Min	Max	Reference
Radius mid-LAD (r_L)[mm]	0.5	3.0	[38]
Radius capillaries (r_c)[μm]	0.5	2.5	[39]
Length mid-LAD (L_L)[cm]	4.0	10	[40,41]

Table A5
Constants used in the numerical models.

Abbreviation	Description	Value	Reference
$\rho_b\left[\frac{kg}{m^3}\right]$	Blood density	1057	[45]
$c_s\left[\frac{J}{kg \cdot K}\right]$	Specific heat saline	4190	[45]
$c_b\left[\frac{J}{kg \cdot K}\right]$	Specific heat blood	3651	[45]
$c_t\left[\frac{J}{kg \cdot K}\right]$	Specific heat tissue	3683	[45]
$k_m\left[\frac{W}{m \cdot kg}\right]$	Thermal conductivity of the myocardium	0.582	[45]
$d_{a0}[m]$	Thickness between artery and ambience. (based on coronary artery wall thickness)	0.001	[46]
$d_{am}[m]$	Thickness between artery and myocardium. (based on left ventricle wall thickness)	0.010	[47]
$d_{av}[m]$	Thickness between artery and vein. (based on coronary artery wall thickness)	0.001	[46]
$d_{m0}[m]$	Thickness between myocardium and ambience. (based on length cardiac myocytes)	0.001	[39]
$d_{mv}[m]$	Thickness between myocardium and vein. (based on left ventricle wall thickness)	0.010	[47]
$d_{v0}[m]$	Thickness between vein and ambience. (based on coronary artery wall thickness)	0.001	[46]

Appendix A. Parameters

The uncertainty range of the parameters in model 1 and 2 are based on literature values and characteristics of the mid-LAD and capillaries assuming that these values are equal for pigs and humans (Table A.3).

Subsequently, the parameters for pigs (Table A.4, column 3) and humans (Table A.4, column 4) are based on these values and the mass of the heart (m_h) (second row in Table A.4, respectively). The m_h of pigs and humans are approximately 500 [31] 300 g [39]. In order to define a range, a deviation of $\pm$33% has been used. There is assumed that 20% of m_h corresponds with the mass of AAR (m). Furthermore, the total volume in the coronary circulation is 1.25 mL, whereof 27.5% corresponds with the coronary arteries (5.5% for mid-LAD), 37.1% with the coronary veins, and 35.4% with the microcirculation. The exchange surface of microcirculation is 500 cm^2 per gram.

Table A4
Minimum and maximum value of the characteristics of mid-LAD and capillaries.

Abbreviation	Parameter	Range pigs	Range humans	Formula	Reference/ Assumption
$m_h[kg]$	Mass heart	[350 650]	[200 400]	–	[37]
$m[kg]$	Mass AAR	[70 130]	[40 80]	$0.2m_h$	–
$A_{a0}[m^2]$	Area between artery and ambience	$[0.63\ 9.42]\cdot10^{-4}$	$[0.63\ 9.42]\cdot10^{-4}$	$\frac{2\pi r_L L_L}{2}$	Half of the artery is in contact with the ambience.
$A_{am}[m^2]$	Area between artery and myocardium (microcirculation)	[1.31 4.06]	[0.75 2.5]	$\frac{500 \pm 125}{2} \cdot 10^{-4}$ per gram	Half of the microcirculation is arterial [40].
$A_{av}[m^2]$	Area between artery and vein	$[0.31\ 4.71]\cdot10^{-4}$	$[0.31\ 4.71]\cdot10^{-4}$	$\frac{2\pi r_L L_L}{4}$	Quarter of the artery is in contact with the vein.
$A_{m0}[m^2]$	Area between myocardium and ambience	$[0.65\ 1.20]\cdot10^{-2}$	$[3.68\ 7.37]\cdot10^{-3}$	$\frac{m_h}{0.01\rho}$	Based on left ventricle wall thickness of 1 cm.
$A_{mv}[m^2]$	Area between myocardium and vein (microcirculation)	[1.31 4.06]	[0.75 2.5]	$\frac{500 \pm 125}{2} \cdot 10^{-4}$ per gram	Half of the microcirculation is venous [37].
$A_{v0}[m^2]$	Area between vein and ambience	$[0.63\ 9.42]\cdot10^{-4}$	$[0.63\ 9.42]\cdot10^{-4}$	$\frac{2\pi r_L L_L}{2}$	Half of the vein is in contact with the ambience.
$V_a[mL]$	Volume artery	[1.01 1.88]	[0.58 1.16]	5.5% $\pm$ 17.7% van 1.25 mL per 100 g	[42,43]
$V_v[mL]$	Volume vein	[2.40 4.45]	[1.37 2.74]	37.1% $\pm$ 17.7% van 1.25 mL per 100 g	[42,43]
$\phi_a[mL/min]$	Flow artery	[50 300]	[50 300]	–	[44]
$\phi_v[mL/min]$	Flow vein	[50 300]	[50 300]	–	[44]

Appendix B. Clinical data of SINTAMI

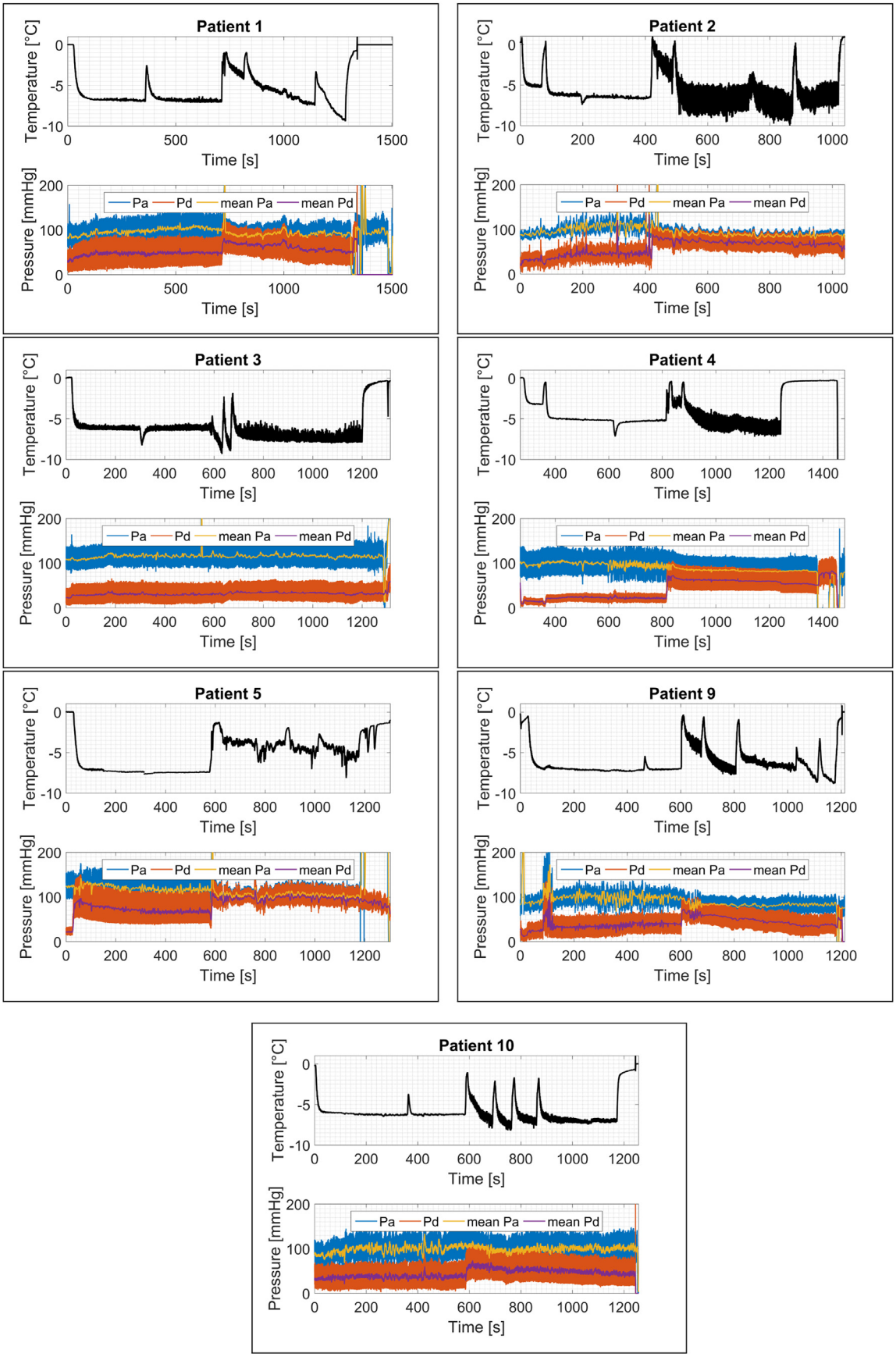

Fig. B6. Arterial temperature data (black) and P_a (blue), mean P_a (yellow), P_d (orange), and mean P_d (purple) data of the SINTAMI study for patients 1-5, 9, and 10. (For interpretation of the references to color in this figure legend, the reader is referred to the web version of this article.)

Appendix C. Simulation of patient data

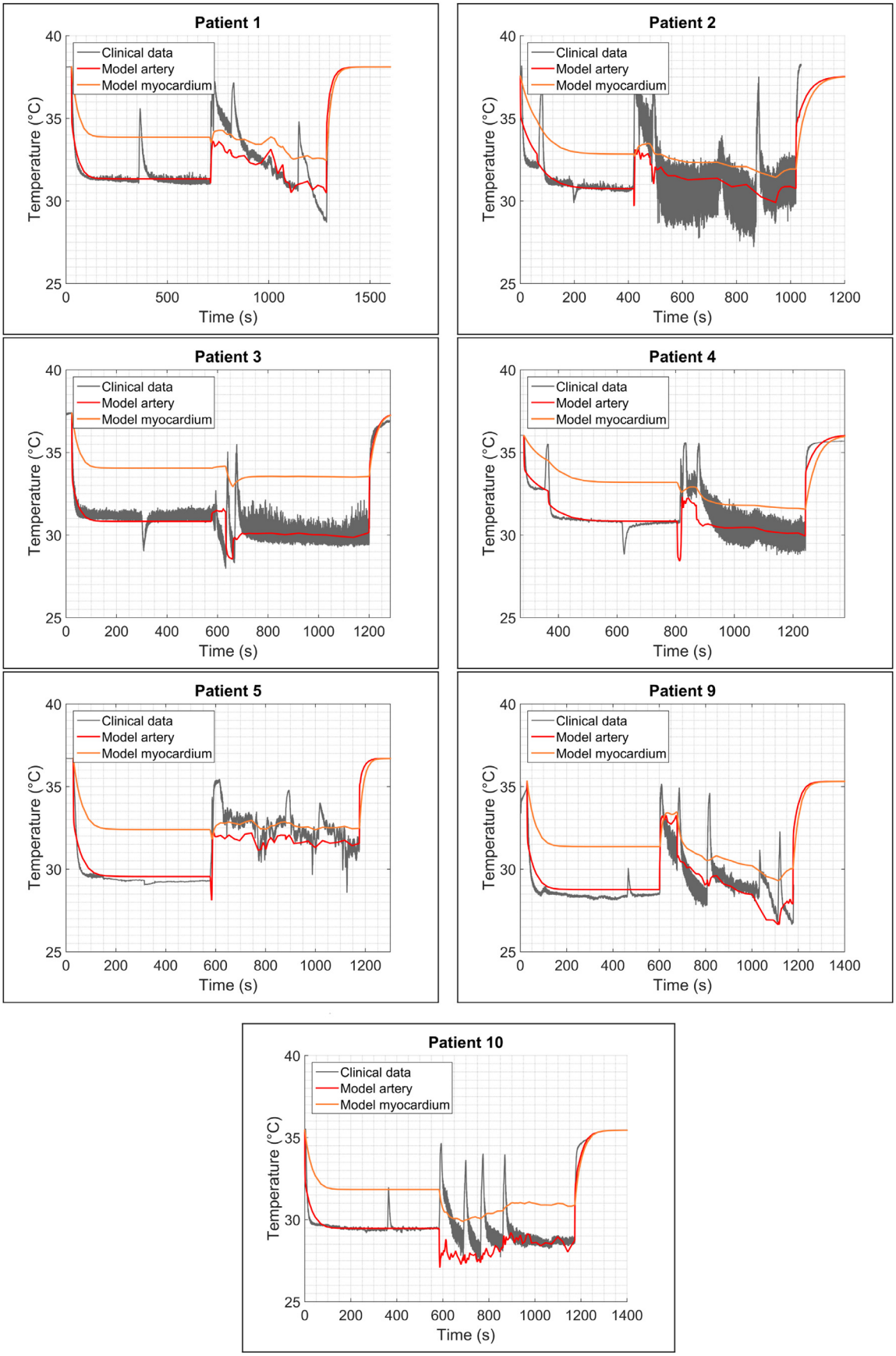

Fig. C7. The intracoronary arterial data (grey), temperature response and the simulation of the intracoronary arterial temperature (red). The prediction of the myocardial (orange) temperature of patients 1-5, 9, and 10. (For interpretation of the references to color in this figure legend, the reader is referred to the web version of this article.)

Table C6
Estimated parameters fitted on the arterial temperature data during occlusion phase of SINTAMI.

	Patient 1	Patient 2	Patient 3	Patient 4	Patient 5	Patient 9	Patient 10
$m[kg]$	$4.00 \cdot 10^{-2}$	$7.16 \cdot 10^{-2}$	$4.16 \cdot 10^{-2}$	$4.98 \cdot 10^{-2}$	$4.00 \cdot 10^{-2}$	$4.09 \cdot 10^{-2}$	$4.00 \cdot 10^{-2}$
$A_{a0}[m^2]$	$6.28 \cdot 10^{-5}$	$1.85 \cdot 10^{-4}$	$6.81 \cdot 10^{-5}$	$1.05 \cdot 10^{-4}$	$6.29 \cdot 10^{-5}$	$7.33 \cdot 10^{-5}$	$6.28 \cdot 10^{-5}$
$A_{am}[m^2]$	$1.01 \cdot 10^{-1}$	$1.51 \cdot 10^{-1}$	$7.09 \cdot 10^{-2}$	$9.34 \cdot 10^{-2}$	$7.34 \cdot 10^{-2}$	$6.16 \cdot 10^{-2}$	$8.98 \cdot 10^{-2}$
$A_{av}[m^2]$	$3.14 \cdot 10^{-5}$	$3.18 \cdot 10^{-5}$	$3.15 \cdot 10^{-5}$	$3.54 \cdot 10^{-5}$	$3.14 \cdot 10^{-5}$	$3.24 \cdot 10^{-5}$	$3.14 \cdot 10^{-5}$
$A_{m0}[m^2]$	$5.31 \cdot 10^{-3}$	$5.13 \cdot 10^{-3}$	$4.92 \cdot 10^{-3}$	$4.73 \cdot 10^{-3}$	$4.86 \cdot 10^{-3}$	$4.75 \cdot 10^{-3}$	$5.18 \cdot 10^{-3}$
$A_{mv}[m^2]$	$2.34 \cdot 10^{-2}$	$3.29 \cdot 10^{-2}$	$6.82 \cdot 10^{-2}$	$2.38 \cdot 10^{-2}$	$1.12 \cdot 10^{-2}$	$2.40 \cdot 10^{-2}$	$2.53 \cdot 10^{-2}$
$A_{v0}[m^2]$	$4.83 \cdot 10^{-4}$	$1.04 \cdot 10^{-4}$	$2.47 \cdot 10^{-4}$	$6.75 \cdot 10^{-5}$	$3.53 \cdot 10^{-4}$	$3.28 \cdot 10^{-4}$	$4.21 \cdot 10^{-4}$
$V_a[mL]$	1.16	1.07	1.16	1.15	1.16	1.16	1.16
$V_v[mL]$	1.37	2.74	1.46	1.39	1.37	1.42	1.37
$\phi_a\left[\frac{mL}{min}\right]$	$2.14 \cdot 10^{2}$	$1.80 \cdot 10^{2}$	$1.50 \cdot 10^{2}$	$1.51 \cdot 10^{2}$	$1.22 \cdot 10^{2}$	$2.18 \cdot 10^{2}$	$1.20 \cdot 10^{2}$
$\phi_v\left[\frac{mL}{min}\right]$	$2.37 \cdot 10^{2}$	$9.13 \cdot 10^{1}$	$2.59 \cdot 10^{2}$	$1.03 \cdot 10^{2}$	$1.18 \cdot 10^{2}$	$9.64 \cdot 10^{1}$	$2.17 \cdot 10^{2}$

References

[1] Gaziano TA. Cardiovascular disease in the developing world and its cost-effective management. Circulation 2005;112(23):3547–53. doi:10.1161/CIRCULATIONAHA.105.591792. http://circ.ahajournals.org/content/112/23/3547.

[2] Go AS, Mozaffarian D, Roger VL, Benjamin EJ, Berry JD, Blaha MJ, et al. Heart disease and stroke statistics 2014 update. Circulation 2014;129(3):e28–e292. doi:10.1161/01.cir.0000441139.02102.80. https://www.ncbi.nlm.nih.gov/pmc/articles/PMC5408159/.

[3] Nabel EG, Braunwald E. A tale of coronary artery disease and myocardial infarction. N Engl J Med 2012;366(1):54–63. doi:10.1056/NEJMra1112570. https://doi.org/10.1056/NEJMra1112570.

[4] Ezekowitz JA, Kaul P, Bakal JA, Armstrong PW, Welsh RC, McAlister FA. Declining in-hospital mortality and increasing heart failure incidence in elderly patients with first myocardial infarction. J Am Coll Cardiol 2009;53(1):13–20. doi:10.1016/j.jacc.2008.08.067. http://www.sciencedirect.com/science/article/pii/S0735109708033159.

[5] Yeh RW, Sidney S, Chandra M, Sorel M, Selby JV, Go AS. Population trends in the incidence and outcomes of acute myocardial infarction. N Engl J Med 2010;362(23):2155–65. doi:10.1056/NEJMoa0908610. https://doi.org/10.1056/NEJMoa0908610.

[6] Kaul P, Ezekowitz JA, Armstrong PW, Leung BK, Savu A, Welsh RC, et al. Incidence of heart failure and mortality after acute coronary syndromes. Am Heart J 2013;165(3):379–385.e2. doi:10.1016/j.ahj.2012.12.005. http://www.sciencedirect.com/science/article/pii/S0002870312008459.

[7] McManus DD, Gore J, Yarzebski J, Spencer F, Lessard D, Goldberg RJ. Recent trends in the incidence, treatment, and outcomes of patients with STEMI and NSTEMI. Am J Med 2011;124(1):40–7. doi:10.1016/j.amjmed.2010.07.023. http://www.sciencedirect.com/science/article/pii/S0002934310007369.

[8] Stone GW, Selker HP, Thiele H, Patel MR, Udelson JE, Ohman EM, et al. Relationship between infarct size and outcomes following primary PCI: patient-level analysis from 10 randomized trials. J Am Coll Cardiol 2016;67(14):1674–83. doi:10.1016/j.jacc.2016.01.069. http://www.sciencedirect.com/science/article/pii/S0735109716007233.

[9] O'Gara PT, Kushner FG, Ascheim DD, Casey DE, Chung MK, Lemos JAd, et al. 2013 ACCF/AHA Guideline for the Management of ST-Elevation Myocardial Infarction: Executive Summary: A Report of the American College of Cardiology Foundation/American Heart Association Task Force on Practice Guidelines. J Am Coll Cardiol 2013;61(4):485–510. doi:10.1016/j.jacc.2012.11.018. http://www.onlinejacc.org/content/61/4/485.

[10] Fordyce CB, Gersh BJ, Stone GW, Granger CB. Novel therapeutics in myocardial infarction: targeting microvascular dysfunction and reperfusion injury. Trends Pharmacol Sci 2015;36(9):605–16. doi:10.1016/j.tips.2015.06.004.

[11] Hausenloy DJ, Botker HE, Engstrom T, Erlinge D, Heusch G, Ibanez B, et al. Targeting reperfusion injury in patients with ST-segment elevation myocardial infarction: trials and tribulations. Eur Heart J 2017;38(13):935–41. doi:10.1093/eurheartj/ehw145.

[12] Yellon DM, Hausenloy DJ. Myocardial reperfusion injury. N Engl J Med 2007;357(11):1121–35. doi:10.1056/NEJMra071667.

[13] Fröhlich GM, Meier P, White SK, Yellon DM, Hausenloy DJ. Myocardial reperfusion injury: looking beyond primary PCI. Eur Heart J 2013;34(23):1714–22. doi:10.1093/eurheartj/eht090.

[14] Kapur NK, Karas RH. A new shield from the double-edged sword of reperfusion in STEMI. Eur Heart J 2015;36(44):3058–60. doi:10.1093/eurheartj/ehv438.

[15] Montecucco F, Carbone F, Schindler TH. Pathophysiology of ST-segment elevation myocardial infarction: novel mechanisms and treatments. Eur Heart J 2016;37(16):1268–83. doi:10.1093/eurheartj/ehv592.

[16] Götberg M, Olivecrona GK, Engblom H, Ugander M, van der Pals J, Heiberg E, et al. Rapid short-duration hypothermia with cold saline and endovascular cooling before reperfusion reduces microvascular obstruction and myocardial infarct size. BMC Cardiovasc Disord 2008;8:7. doi:10.1186/1471-2261-8-7.

[17] Dae MW, Gao DW, Sessler DI, Chair K, Stillson CA. Effect of endovascular cooling on myocardial temperature, infarct size, and cardiac output in human-sized pigs. Am J Physiol Heart Circ Physiol 2002;282(5):1584–91. doi:10.1152/ajpheart.00980.2001.

[18] Duncker DJ, Klassen CL, Ishibashi Y, Herrlinger SH, Pavek TJ, Bache RJ. Effect of temperature on myocardial infarction in swine. Am J Physiol 1996;270(4 Pt 2):H1189–99.

[19] Erlinge D. A review of mild hypothermia as an adjunctive treatment for ST-elevation myocardial infarction. Ther Hypothermia Temp Manag 2011;1(3):129–41. doi:10.1089/ther.2011.0008.

[20] Hale SL, Dave RH, Kloner RA. Regional hypothermia reduces myocardial necrosis even when instituted after the onset of ischemia. Basic Res Cardiol 1997;92(5):351–7.

[21] Hale SL, Kloner RA. Myocardial temperature in acute myocardial infarction: protection with mild regional hypothermia. Am J Physiol 1997;273(1 Pt 2):H220–7.

[22] Hale SL, Kloner RA. Myocardial temperature reduction attenuates necrosis after prolonged ischemia in rabbits. Cardiovasc Res 1998;40(3):502–7. doi:10.1016/S0008-6363(98)00191-6. https://academic.oup.com/cardiovascres/article/40/3/502/275284/Myocardial-temperature-reduction-attenuates.

[23] Erlinge D, Götberg M, Noc M, Lang I, Holzer M, Clemmensen P, et al. Therapeutic hypothermia for the treatment of acute myocardial infarction-combined analysis of the RAPID MI-ICE and the CHILL-MI trials. Ther Hypothermia and Temp Manag 2015;5(2):77–84. doi:10.1089/ther.2015.0009.

[24] Erlinge D, Götberg M, Lang I, Holzer M, Noc M, Clemmensen P, et al. Rapid endovascular catheter core cooling combined with cold saline as an adjunct to percutaneous coronary intervention for the treatment of acute myocardial infarction. The CHILL-MI trial: a randomized controlled study of the use of central venous catheter core cooling combined with cold saline as an adjunct to percutaneous coronary intervention for the treatment of acute myocardial infarction. J Am Coll Cardiol 2014;63(18):1857–65. doi:10.1016/j.jacc.2013.12.027.

[25] Götberg M, Olivecrona GK, Koul S, Carlsson M, Engblom H, Ugander M, et al. A pilot study of rapid cooling by cold saline and endovascular cooling before reperfusion in patients with st-elevation myocardial infarctionclinical perspective. Circ Cardiovasc Interv 2010;3(5):400–7. doi:10.1161/CIRCINTERVENTIONS.110.957902. http://circinterventions.ahajournals.org/content/3/5/400.

[26] Kandzari DE, Chu A, Brodie BR, Stuckey TA, Hermiller JB, Vetrovec GW, et al. Feasibility of endovascular cooling as an adjunct to primary percutaneous coronary intervention (results of the LOWTEMP pilot study). Am J Cardiol 2004;93(5):636–9. doi:10.1016/j.amjcard.2003.11.038.

[27] Nichol G, Strickland W, Shavelle D, Maehara A, Ben-Yehuda O, Genereux P, et al. VELOCITY Investigators, Prospective, multicenter, randomized, controlled pilot trial of peritoneal hypothermia in patients with ST-segment-elevation myocardial infarction. Circ Cardiovasc Interv 2015;8(3):e001965. doi:10.1161/CIRCINTERVENTIONS.114.001965.

[28] Villablanca PA, Rao G, Briceno DF, Lombardo M, Ramakrishna H, Bortnick A, et al. Therapeutic hypothermia in ST elevation myocardial infarction: a systematic review and meta-analysis of randomised control trials. Heart (Br Cardiac Soc) 2016;102(9):712–19. doi:10.1136/heartjnl-2015-308559.

[29] Otterspoor LC, van Nunen LX, van 't Veer M, Johnson NP, Pijls NHJ. Intracoronary hypothermia before reperfusion to reduce reperfusion injury in acute myocardial infarction: a novel hypothesis and technique. Ther Hypothermia Temp Manag 2017;7(4):199–205. doi:10.1089/ther.2017.0006.

[30] Otterspoor LC, van't Veer M, van Nunen LX, Wijnbergen I, Tonino PAL, Pijls NH. Safety and feasibility of local myocardial hypothermia: intracoronary hypothermia in acute myocardial infarction. Catheter Cardiovasc Interv 2016;87(5):877–83. doi:10.1002/ccd.26139. http://doi.wiley.com/10.1002/ccd.26139.

[31] Otterspoor LC, van Nunen LX, Rosalina TT, Veer MV, Tuijl SV, Stijnen M, et al. Intracoronary hypothermia for acute myocardial infarction in the isolated beating pig heart. Am J Transl Res 2017b;9(2):558–68.

[32] de Hart J, de Weger A, van Tuijl S, Stijnen JMA, van den Broek CN, Rutten MCM, et al. An ex vivo platform to simulate cardiac physiology: a new dimension for therapy development and assessment. Int J Artif Organs 2011;34(6):495–505. doi:10.5301/IJAO.2011.8456.

[33] Otterspoor LC, van't Veer M, van Nunen LX, Brueren GRG, Tonino PAL, Wijnbergen IF, Helmes H, Zimmermann FM, Van Hagen E, Johnson NP, Pijls NHJ. Safety and feasibility of selective intracoronary hypothermia in acute myocardial infarction. EuroIntervention 2017;13(12):1475–82.

[34] Saltelli A, Ratto M, Andres T, Campolongo F, Cariboni J, Gatelli D, et al. Global sensitivity analysis: the primer. John Wiley & Sons; 2008. ISBN 978-0-470-72517-7.

[35] Sobol IM. Global sensitivity indices for nonlinear mathematical models and their Monte Carlo estimates. Math Comput Simul 2001;55(13):271–80. doi:10.1016/S0378-4754(00)00270-6. http://www.sciencedirect.com/science/article/pii/S0378475400002706.

[36] Saltelli A. Making best use of model evaluations to compute sensitivity indices. Comput Phys Commun 2002;145(2):280–97. doi:10.1016/S0010-4655(02)00280-1. http://www.sciencedirect.com/science/article/pii/S0010465502002801.

[37] Bassingthwaighte JB, Yipintsoi T, Harvey RB. Microvasculature of the dog left ventricular myocardium. Microvasc Res 1974;7(2):229–49. doi:10.1016/0026-2862(74)90008-9. http://www.sciencedirect.com/science/article/pii/0026286274900089.

[38] Douglas PS, Fiolkoski J, Berko B, Reichek N. Echocardiographic visualization of coronary artery anatomy in the adult. J Am Coll Cardiol 1988;11(3):565–71. doi:10.1016/0735-1097(88)91532-X. http://www.sciencedirect.com/science/article/pii/073510978891532X.

[39] Boron WF, Boulpaep EL. Medical physiology. Elsevier Health Sciences; 2016. ISBN 978-1-4557-3328-6.

[40] van der Horst A, Boogaard FL, van't Veer M, Rutten MCM, Pijls NHJ, van de Vosse FN. Towards patient-specific modeling of coronary hemodynamics in healthy and diseased state. Comput Math Methods Med 2013;2013:e393792. doi:10.1155/2013/393792. http://www.hindawi.com/journals/cmmm/2013/393792/abs/.

[41] Kenner PDT. The measurement of blood density and its meaning. Basic Res Cardiol 1989;84(2):111–24. doi:10.1007/BF01907921. http://link.springer.com/article/10.1007/BF01907921.

[42] Arts MGJ. A mathematical model of the dynamics of the left ventricle and the coronary circulation. Rijksuniversiteit Limburg; 1978. https://cris.maastrichtuniversity.nl/portal/en/publications/a-mathematical-model-of-the-dynamics-of-the-left-ventricle-and-the-coronary-circulation(b8c6389c-29e5-41d5-bdf0-83b851d99852).html.

[43] Kassab GS, Lin DH, Fung YC. Morphometry of pig coronary venous system. Am J Physiol Heart Circ Physiol 1994;267(6):H2100–13. http://ajpheart.physiology.org/content/267/6/H2100.

[44] Aarnoudse W, van 't Veer M, Pijls NHJ, ter Woorst J, Vercauteren S, Tonino P, et al. Direct volumetric blood flow measurement in coronary arteries by thermodilution. J Am Coll Cardiol 2007;50(24):2294–304. doi:10.1016/j.jacc.2007.08.047. http://www.sciencedirect.com/science/article/pii/S0735109707029907.

[45] Mcintosh RL, Anderson V. A comprehensive tissue properties database provided for the thermal assessment of a human at rest. Biophys Rev Lett 2010;05(03):129–51. doi:10.1142/S1793048010001184. http://www.worldscientific.com/doi/abs/10.1142/S1793048010001184.

[46] Gradus-Pizlo I, Bigelow B, Mahomed Y, Sawada SG, Rieger K, Feigenbaum H. Left anterior descending coronary artery wall thickness measured by high-frequency transthoracic and epicardial echocardiography includes adventitia. Am J Cardiol 2003;91(1):27–32.

[47] Troy BL, Pombo J, Rackley CE. Measurement of left ventricular wall thickness and mass by echocardiography. Circulation 1972;45(3):602–11. doi:10.1161/01.CIR.45.3.602. http://circ.ahajournals.org/content/45/3/602.